# DESIGNING OF AN OFF-GRID REVERSIBLE HEAT PUMP/ORGANIC RANKINE CYCLE SYSTEM FOR ELECTRICITY AND COOLING DEMANDS OF A NIGERIAN FAMILY FARM

Bentao Guo[1]*, Vincent Lemort[2]

[1]Thermodynamics Laboratory, University of Liege, 4000 Liege, Belgium

[2]Thermodynamics Laboratory, University of Liege, 4000 Liege, Belgium

*Corresponding Author: Bentao.Guo@uliege.be

## ABSTRACT

As renewable energy sources experience rapid growth and widespread adoption worldwide, the pressing challenge lies in efficiently storing and utilizing them. The Carnot battery emerges as a promising solution to this challenge. Existing Carnot batteries based on the Organic Rankine Cycle (ORC) mainly focus on district heating and power generation applications but neglect the unique operational conditions found on farms. This study investigates a family farm in Nigeria. Due to the intermittent nature of the national grid, the family relies on diesel generators as a backup power source, thus prompting consideration of renewable energy sources for environmental and energy-saving purposes. Therefore, an off-grid reversible heat pump (HP) /ORC with a photovoltaic (PV) array must be designed to meet the electricity and cooling needs of the farm. The configuration and working fluid of the reversible HP/ORC system are first selected, and then the pinch point and glides of heat exchangers, the top temperature of hot storage, and the built-in volume ratio of the scroll machine are determined. The results give the round-trip efficiency and operating mode details in various demand coverage throughout the year in addition to the COP of HP, and ORC efficiency at nominal conditions. The design with an electrical heater and ice-cooled ORC is proposed to improve system performance and its COP and ORC efficiency can reach 2.72 and 9.51%, respectively.

## 1 INTRODUCTION

Global warming has become an important concern worldwide, prompting international agreements such as the Kyoto Protocol (United Nations, 1998) and the Paris Agreement (UNFCCC, 2018). In response, nations are urged to curb $CO_2$ emissions and transition towards decarbonization through enhanced energy efficiency and reduced fossil fuel consumption. Renewable energy and energy storage technologies play pivotal roles in this transition, offering alternatives to traditional grid reliance and fossil fuel dependency for electricity generation. The Carnot battery, a power-to-heat-to-power technology, is gaining prominence for its ability to store electricity as heat energy and subsequently regenerate electricity using a heat engine when needed (Dumont et al., 2023). Compared to lithium battery (Smith et al, 2017), it has advantages: longer lifetime, greener, and more suitable for large-scale applications (Martinek et al, 2023; Benato and Stoppato, 2018).

Carnot batteries utilizing HP/ORC have been mainly applied in electricity storage and district heating applications (Poletto et al., 2024; Scharrer et al., 2022). Among these, reversible HP/ORC systems have attracted attention for their simplified design and application versatility (Dumont and Lemort, 2019). By employing reversible volumetric machines and heat exchangers, these systems offer a simplified approach to electricity storage and generation, reducing the need for redundant components (Dumont et al., 2020; Torricelli et al., 2023; Tassenoy et al., 2022; Steger et al., 2020; Dumont and Lemort, 2020a). Despite advancements, previous research has predominantly focused on applying reversible HP/ORC systems in small-scale building heating/electricity generation (Dumont et al.,

2023), neglecting the unique operational conditions encountered on farms, which have the cooling demand for food preservation in a low-temperature range, and the possibility of off-grid conditions.

Therefore, this study aims to design a Carnot battery integrated with renewable energy sources tailored to the needs of a Nigerian family farm, providing a sustainable solution to meet the farm's electrical and cooling demands, and eliminating dependence on the grid and reliance on diesel generators. Sector 2 introduces the specific characteristics of the farm, while Sector 3 outlines the design model and preliminary operating conditions. Sector 4 details the design process, including optimal pinch point, top temperature of hot storage, glides, and build-in volume ratio of reversible scroll machine, and analyzes the effect of demand coverage on sizing. In this sector, an improvement design is proposed with an electrical heater, and its performance is also gained. Finally, under optimal design and sizing, the whole-year performance is presented.

## 2    CASE DESCRIPTION

The study focuses on a small-scale family farm situated in Eruemukohwarien, Delta State, Nigeria. The farm is involved in various agricultural activities, including cassava, yam, corn cultivation, fish farming, and vegetable cultivation. Consequently, the farm's operations require electrical demands for irrigation pumps and light bulbs and cooling demands for food preservation. Based on collected data, irrigation pumps are operated between 9:00 and 13:00, requiring a power of 26.68 kW. Light bulbs are utilized from 18:00 to 8:00, with a power consumption of 1.46 kW. Additionally, the farm necessitates continuous cooling demand for food preservation, with the cold room maintaining a temperature range of 0-5°C and a power requirement ($\dot{W}_{cooling}$) of 14 kW, as illustrated in Figure 1.
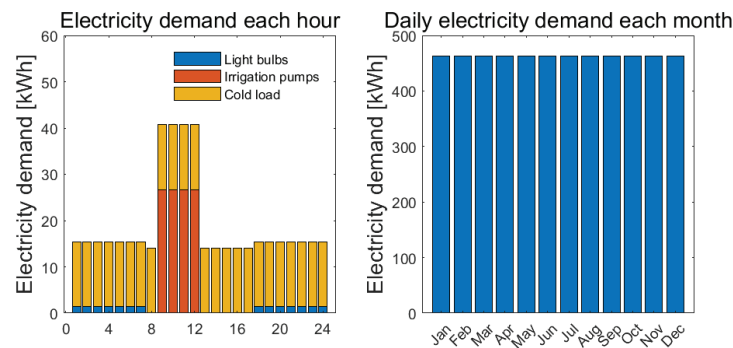


Figure 1. Electricity demands every day and every month

Given the low-temperature requirement for food preservation, ice latent storage has become a feasible solution for achieving low-temperature storage. The ice storage system is integrated with a cooling coil inside the cold room through a glycol-water circuit. Considering the purpose of the off-grid status, a combination of PV panels and a Carnot battery is designed to meet the farm's entire electrical demands. The available land area for renewable energy installation is 10,000 m$^2$. The schematic of the reversible HP/ORC system combined with PV is depicted in Figure 2. In the HP mode, the working fluid undergoes compression by the compressor, subsequently heating the hot water in the condenser (HPHX). Following this, the cooled working fluid is expanded by the expansion valve (TXV), absorbing heat from the glycol-water solution in the evaporator (LPHX). In the ORC mode, the working fluid absorbs heat from hot water in the evaporator (HPHX), vaporizing in the process. Upon expansion in the expander, the vapor converts thermal energy into power, which is then cooled and condensed by the glycol water in the condenser (LPHX), before being pumped back to the evaporator (HPHX). A liquid receiver (LR) is positioned before the expansion valve to store non-circulating working fluid. A hot water storage (a thermocline single tank system) is employed to facilitate high-temperature storage. Since the counter-flow between two fluids in heat exchangers (HPHX, LPHX) must be ensured, considering the change in the direction of the working fluid between HP and ORC modes, the flow direction of the secondary fluid must also change accordingly (Dumont, 2017). To achieve this, a four-way valve is installed in the hot water loop. During HP operation, if the cooling

37$^{th}$ INTERNATIONAL CONFERENCE ON EFFICIENCY, COST, OPTIMIZATION, SIMULATION AND ENVIRONMENTAL IMPACT OF ENERGY SYSTEMS, 30 JUNE - 4 JULY, 2024, RHODES, GREECE

431

capacity exceeds the cooling demand, the glycol water from the evaporator simultaneously charges the ice storage and cools the food. Conversely, if the cooling demand surpasses the cooling capacity, both the glycol water from the evaporator and the ice storage work together to cool the food. Additionally, to accommodate the directional changes during the charging and discharging of the ice storage tank, a four-way valve is also installed in this loop.
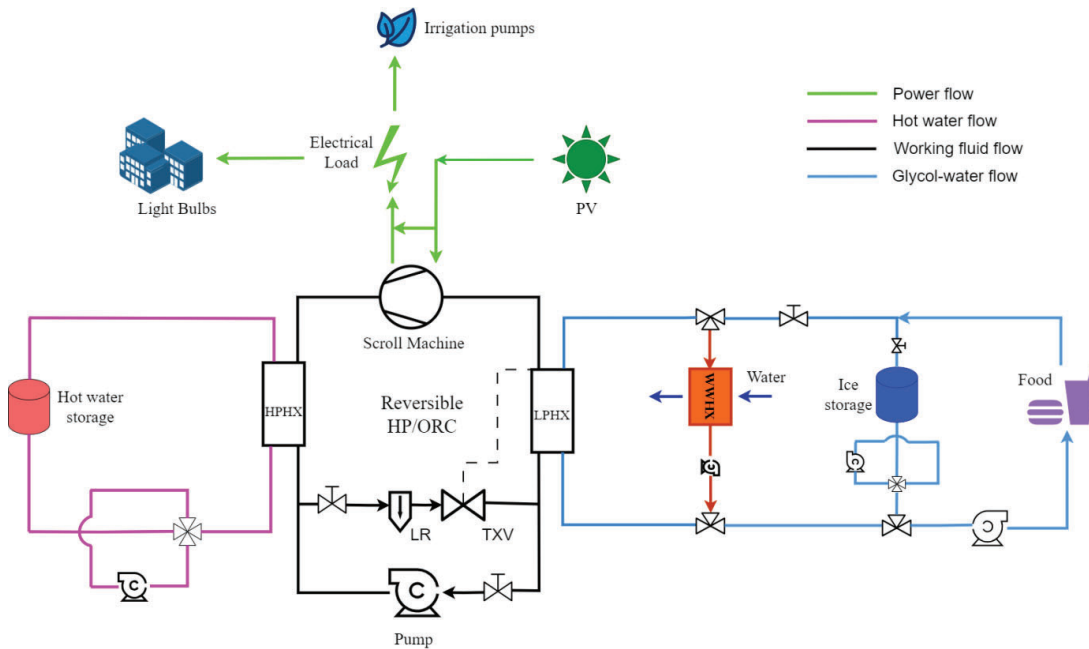


Figure 2. Schematic of the configuration of reversible HP/ORC with PV

## 3 METHODOLOGY

Designing model is fully built in MATLAB environment. The model of reversible HP/ORC refers to Dumont et al (2023), and other models are presented in sections 3.1-3.4. The time step is set as 1 hour.

### 3.1 PV array model
Yearly outputs of the PV system are based on the yearly meteorological condition data of the farm location, which is provided by the Meteonorm software. The equation of power of the PV array refers to Migliari et al (2024):

$$\dot{W}_{PV,tot} = \dot{W}_{PV} \times \eta_{inv} \times f_{PV} \times N_{PV} \tag{1}$$

$\dot{W}_{PV}$ is the power of each PV panel calculated by:

$$\dot{W}_{PV} = \frac{\dot{W}_{PV,peak} \times [1 + \alpha \times (T_{cell} - T_{cell,STC})] \times GI}{GI_{STC}} \tag{2}$$

$T_{cell}$ can be calculated according to Migliari et al (2024), and $N_{PV}$ can be calculated by the equation:

$$N_{PV} = \frac{\dot{W}_{PV,nom}}{\dot{W}_{PV,STC}} \tag{3}$$

Thus, the total area of the PV array can be gained by:

$$A_{PV,tot} = N_{PV} \times A_{PV} \tag{4}$$

### 3.2 Mode switching model
Electricity power demand for the Carnot battery in this case is:

$$\dot{W}_{CB} = \dot{W}_{load} - \dot{W}_{PV,tot} \tag{5}$$

Where $\dot{W}_{load}$ is the sum of electricity power of irrigation pumps and light bulbs.
If $\dot{W}_{CB} > 0$, ORC mode is on (HP off), and electricity demand for ORC is:

$$\dot{W}_{ORC} = \dot{W}_{CB}, if \ \dot{W}_{CB} > 0 \tag{6}$$

$$\dot{W}_{ORC} = 0, if \ \dot{W}_{CB} \leq 0 \tag{7}$$

If $\dot{W}_{CB} < 0$, HP mode is on (ORC off), and electricity power available for HP consumption is:

$$\dot{W}_{HP} = \dot{W}_{PV,tot} - \dot{W}_{load} \tag{8}$$

As for the cooling demand, in this case, it will be covered by the designed system totally without extra refrigerators, so the cooling demand is calculated by:

$$\dot{Q}_{load} = EER \times \dot{W}_{cooling} \tag{9}$$

Where, EER is the energy efficiency ratio of cooling equipment used for the cold room in the farm at present, and it is assumed to be 50% of the inverse Carnot efficiency. Hence, EER is 2.73 in this case.

### 3.3 Hot water storage model

Variation of hot water storage capacity each hour is calculated by:

$$\Delta E_{hot,sto} = \int_0^{3600} (\dot{Q}_{HP,cd} - \dot{Q}_{ORC,ev}) dt \tag{10}$$

The total mass of hot water needed can be calculated by:

$$M_{hot,sto} = \frac{E_{hot,sto}}{c_w \times \Delta T_{hot,w}} \tag{11}$$

### 3.4 Ice storage model

Cooling energy for a cold room each hour can be gained by:

$$E_{cooling} = \int_0^{3600} \dot{Q}_{load} dt \tag{12}$$

Like hot storage, the variation of ice storage capacity each hour is calculated by:

$$\Delta E_{ice,sto} = \int_0^{3600} (\dot{Q}_{HP,ev} - \dot{Q}_{cooling}) dt \tag{13}$$

The total mass of ice needed here can be calculated by:

$$M_{ice,sto} = \frac{E_{ice,sto}}{L_w} \tag{14}$$

### 3.5 Preliminary condition setting

In this case study, a variable-speed reversible scroll machine is used to meet various farm demands and fit various PV supplies. A preliminary design condition should be set to start the simulation to select the proper working fluid, as presented in Table 1. The pinch points of each heat exchanger are kept identical. For ORC, in the water-water heat exchanger (WWHX), the minimum temperature difference between glycol-water and well water of WWHX is set at 5 K. Average temperature of well water here is 27.3 °C, and the glycol-water supply temperature of ORC condenser is 32.3 °C. In HP mode, the glycol-water temperature is a little lower than the food preservation room temperature, so the glycol-water exhaust temperature of the HP evaporator is -1 °C.

**Table 1:** Preliminary condition details

| Parameters | Value |
|---|---|
| Hot water exhaust temperature of HP condenser [C] | 80 |
| Hot water exhaust temperature of ORC evaporator [C] | 65 |
| Glycol-water exhaust temperature of HP evaporator [C] | -1 |
| Glycol-water exhaust temperature of ORC condenser [C] | 32.3 |
| Scroll machine isentropic efficiency [-] | 0.7 |
| Pump efficiency [-] | 0.5 |
| Pinch point of heat exchangers [K] | 5 |
| Superheating / Subcooling degree [K] | 5 / 5 |
| The maximum speed of the compressor [rpm] | 6000 |
| The maximum speed of the expander [rpm] | 4000 |

37th INTERNATIONAL CONFERENCE ON EFFICIENCY, COST, OPTIMIZATION, SIMULATION AND ENVIRONMENTAL IMPACT OF ENERGY SYSTEMS, 30 JUNE - 4 JULY, 2024, RHODES, GREECE

433

## 4    RESULTS AND ANALYSIS

### 4.1    Performance criteria

In this case, cooling demand is satisfied by ice storage or HP directly, without extra refrigeration equipment driven by electricity, so round-trip efficiency here is defined as:

$$RTE = \frac{W_{ORC} + E_{cooling}/EER}{W_{HP}} \qquad (15)$$

Where $E_{cooling}/EER$ is the cold room electricity consumption saved by ice storage and HP cooling.
COP and $\eta_{ORC}$ are used to evaluate the HP and ORC performance in nominal conditions, respectively:

$$COP = \frac{\dot{Q}_{HP,cd}}{\dot{W}_{HP}} \qquad (16)$$

$$\eta_{ORC} = \frac{\dot{W}_{ORC}}{\dot{Q}_{ORC,ev}} \qquad (17)$$

Where, $\dot{W}_{HP}$ and $\dot{W}_{ORC}$ are HP power consumption rate (total consumption of compressor and pumps) and ORC power generation rate (expander power production minus total consumption of the working-fluid pump and secondary-fluid pumps), respectively. To evaluate the match of reversible components while designing the reversible HP/ORC, the ratio of Reynolds number is introduced (Dumont and Lemort, 2020b) as equation (18). It is defined as the ratio of the highest Reynolds number of ORC (exhaust of the expander) divided by the highest one of HP (supply of the compressor). If its value is closer to one, they match better.

$$R_{Re} = \frac{Re_{exp,ex}}{Re_{cmp,su}} \qquad (18)$$

### 4.2    Yearly renewable energy power

The power of PV panels is an essential input for reversible HP/ORC design. The solar irradiance on panels and $\dot{W}_{PV}$ in one year are shown in Fig.3. For instance, at around 4500h and 6500h, solar irradiance is lower, so if the sizing of PV and Carnot battery covers demands during these hours, they will be oversized in other hours during the year.
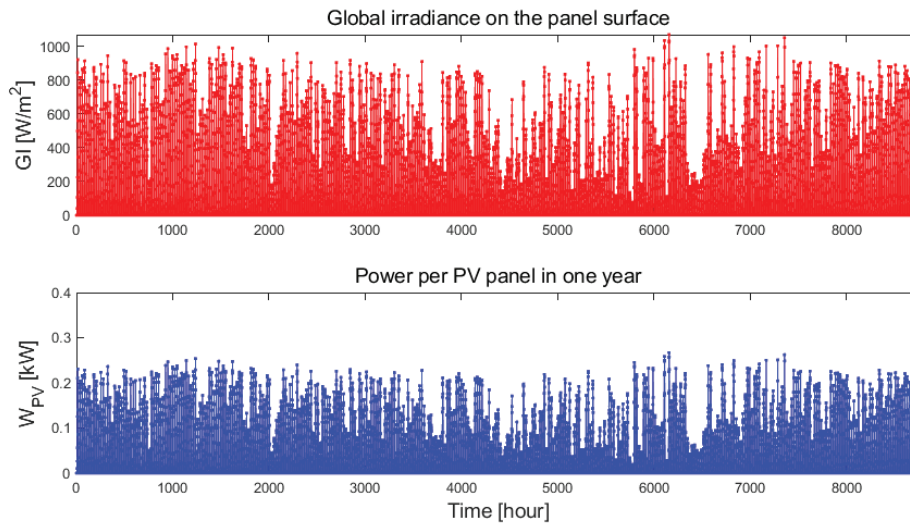


Figure 3. Solar irradiance and power per PV panel ($P_{PV}$) in one year

### 4.3    Working fluid selection

To design a sub-critical cycle, the critical temperature must be higher than the compressor outlet temperature. Besides, the HP evaporation temperature will be lower than -1 ℃, so the working fluid must have a decent cooling performance at this temperature. Refrigerants' effect on the environment must also be considered. Therefore, the working fluid selection criteria are: 1) its critical temperature is higher than 90℃; 2) its nominal boiling temperature is lower than 0 ℃; 3) its ODP should be 0 and its GWP should be less than 150. Hence, R1234ze(E), R1233zd(E), R1234yf, and R152a are taken

into consideration, and a more detailed simulation result is shown in Figure 4, which is the variation of COP, $\eta_{ORC}$ and $R_{Re}$ with the build-in volumetric ratio ($R_V$). $R_V$ is a geometric parameter of a scroll machine, and its definition has been discussed in previous research by Lemort et al (2009). In this case study, R152a is the optimal choice for reversible HP/ORC as it has the highest COP in all $R_V$ and the highest $\eta_{ORC}$ when $R_V$ is low. Its $R_{Re}$ is lower than R1233ze(E) and is like other fluids. Therefore, the following analyses are all conducted with R152a as the working fluid.
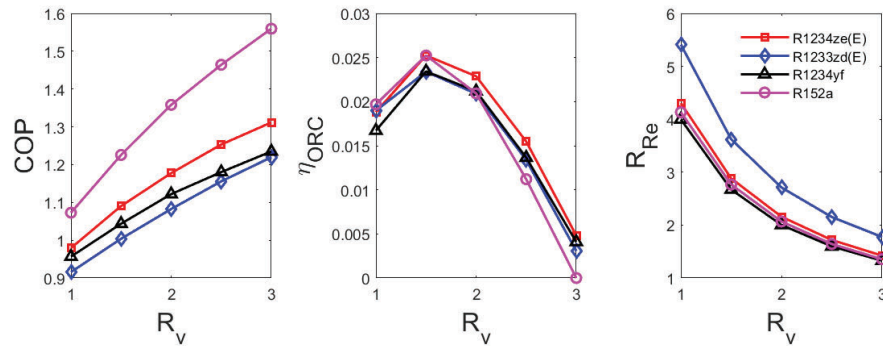


Figure 4. Comparison of various working fluids

## 4.4    Effect of pinch and secondary fluid temperature/glide

The average temperature difference between the working fluid and the secondary fluid (hot water/glycol-water) will vary with the pinch of heat exchangers and their glides. The glide of hot water in the HP condenser and ORC evaporator remains fixed at the same value. If the hot water supply temperature of the ORC evaporator is set as $T_{hot}$, the hot water supply temperature of the HP condenser will be $T_{hot}$ minus its glide. Similarly, the temperature of glycol water entering the ice storage is fixed at -1°C, with the glycol-water supply temperature of the HP evaporator being this value (-1°C) plus its glide. As the HP performance improves with the increase of its evaporation temperature, this glide value should be as low as possible, so it is set as 5K.

$T_{hot}$, hot water glide and glycol-water glide of the ORC condenser will be discussed here. $R_V$ here is set at 1.6 because its optimal $R_V$ is between 1.5 and 2.0 as shown in Figure 4. Under the condition of Table 1, the minimum swept volume of the compressor ($V_{S,cmp}$) is the value that can ensure the nominal power of ORC is over the peak power demand and the nominal cooling rate of HP is over the hourly cooling demand, simultaneously. Therefore, $V_{S,cmp}$ is set as 1300 cm$^3$ here. Hot / ice storage capacity and PV nominal power are set large enough to make sure that demands are covered. The variation of COP and $\eta_{ORC}$ with pinch is depicted in Figure 5 (a). Lower pinch results in better performance, but the pinch cannot be too small considering the practical design and fabrication constraints of plate heat exchangers. Therefore, a value of 5K is deemed appropriate for the pinch in this scenario.

With the given pinch=5K, COP and $\eta_{ORC}$ with $T_{hot}$, hot water glide and ORC glycol-water glide are shown in Figure 5 (b-d). As heat pump COP is not impacted by ORC glycol-water glide and its evaporation pressure is determined by the ice storage condition, COP is only influenced by $T_{hot}$ and hot water glide due to the variation of the HP condensation pressure. When $T_{hot}$ is within [80°C,88°C] and hot water glide is within [14K,20K], the HP can reach a decent COP value (>1.1). As for the variation of $\eta_{ORC}$ with various parameters in (c) and (d), if it reaches a satisfactory value (>3%), $T_{hot}$ should be within [86°C,94°C] and hot water glide should be within [10K,16K]. In total, $T_{hot}$ is designed at 87°C, and hot water glide is designed at 15K. Regarding the glycol-water glide of ORC, $\eta_{ORC}$ doesn't drop distinctly when it rises from 5K to 8K, but the glycol water flow rate can drop obviously, so it is designed as 8K.

## 4.5    Effect of parameters of a scroll machine

In a reversible HP/ORC system, the reversible machine plays a key role in ensuring stable operation in both modes. Based on the nominal condition designed from section 4.4, the impact of $R_V$ of the reversible scroll machine is shown in Figure 6. As for the expander, its pressure ratio is 1.73, as a result, its optimal RV is within [1.7,1.8] where its highest expander efficiency appears (Figure 6. b)

without under/over expansion. With higher $R_V$, the COP of HP grows steadily, because the pressure ratio of the compressor is 13.5 due to its high-temperature lift. Therefore, the efficiency of the compressor is low within the given $R_V$ range, and its optimal value of 0.7 happens when $R_V=12.5$ without under/over compression. Hence, $R_V$ is designed as 2.0 here from the aspect of the overall performance of the reversible HP/ORC.
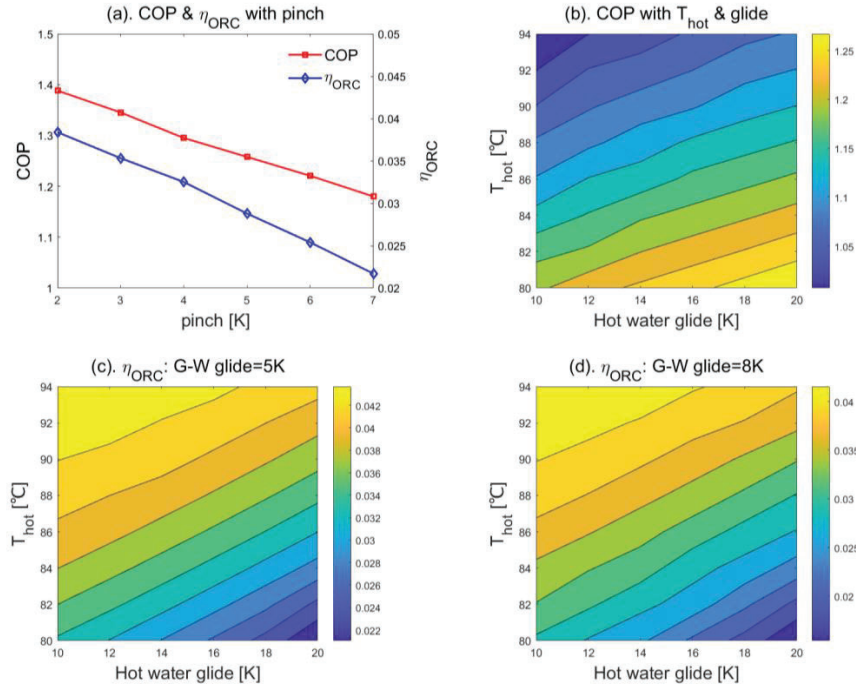


Figure 5. Variation of COP and $\eta_{ORC}$ with $T_{hot}$, pinch, and glides
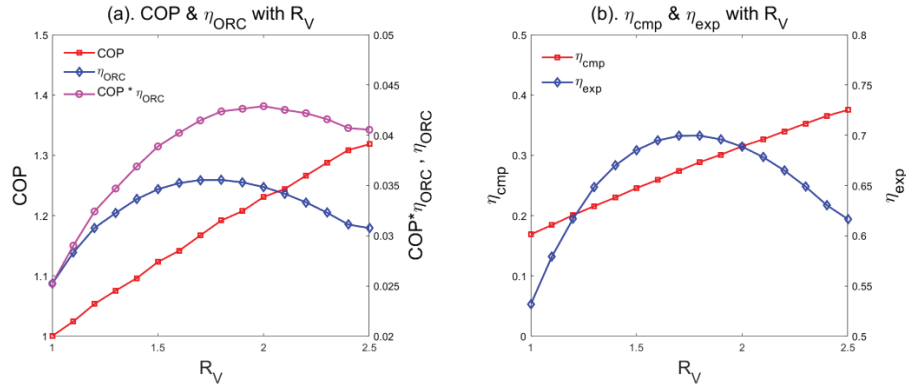


Figure 6. Variation of COP, $\eta_{ORC}$, and compressor/expander efficiency with $R_V$

### 4.6    Effect of coverage for demands

Based on the optimal parameters designed above, the size of reversible HP/ORC, hot storage, ice storage, and PV array should be determined. If the designed system in this off-grid study covers the electricity-cooling demand totally, the system must be oversized, as solar irradiation is too low in some hours over one year (Figure 3), so a large-size PV array and Carnot battery are requested for 100% coverage for demands. If the system is sized for part coverage considering lower investment costs, the farm can use grid or diesel generators when the system cannot satisfy demands. A feasible sizing plan with various coverage is listed in Table 2 (No.1-No.7 without EH). The yearly electricity coverage ($CR_{elec}$) and cooling coverage ($CR_{cooling}$) are defined as below:

436

$$CR_{elec} = \frac{W_{ORC} + W_{PV,load}}{W_{load}} \tag{19}$$

$$CR_{cooling} = \frac{E_{HP,ev}}{E_{cooling}} \tag{20}$$

Where, $W_{ORC}$ and $W_{PV,\,load}$ is electricity energy supplied by ORC and PV array for the electricity load in one year, respectively. $E_{HP,ev}$ represents the yearly cooling energy supplied by HP. $W_{load}$ and $E_{cooling}$ are yearly demands of electricity and cooling, respectively. Under different coverage, performance and rough economic comparisons are shown in Figure 7. Most of the electricity demand is satisfied by PV. The effectiveness ratio of PV power ($R_{PV}$) is the ratio of $W_{PV,\,load}$ and $W_{PV,\,tot}$, representing the effective percentage used for the load of total PV power. Levelized cost of storage (LCOS) is defined in equation (21) to evaluate the average cost of their production, including $W_{PV,\,load}$, $W_{ORC,}$ and $E_{HP,ev}$/ EER, which represents the sum of electricity generated and electricity saved. The investment cost consists of PV panel cost ($C_{PV}$, the Danish Energy Agency), Carnot battery cost ($C_{CB}$, Laterre et al, 2024), hot storage cost ($C_{hot}$, Iqbal, et al., 2023), and ice storage cost ($C_{ice}$, Song, et al, 2018):

$$LCOS = \frac{C_{PV} + C_{CB} + C_{hot} + C_{ice}}{W_{ORC} + W_{PV,load} + E_{HP,ev}/EER} \tag{21}$$

Obviously, in No.7, $R_{PV}$ is low, meaning that the system is oversized, especially the PV array. The PV panel price is high, so from No.6 to No.7, LCOS has a significant lift by 15% and RTE has an apparent reduction from 0.1873 to 0.1266. From No.1 to No.2, where only the size of the scroll machine increases, RTE remains unchanged and LCOS reduces because the lift of $C_{CB}$ is lower than the lift of $E_{HP,ev}$. Similarly from No.5 to No.6, the size of the scroll machine and hot storage increases, but RTE and LCOS are better, as a result of the significant lift of $E_{HP,ev}$. Therefore, PV array size has the largest effect on the performance of the designed system.
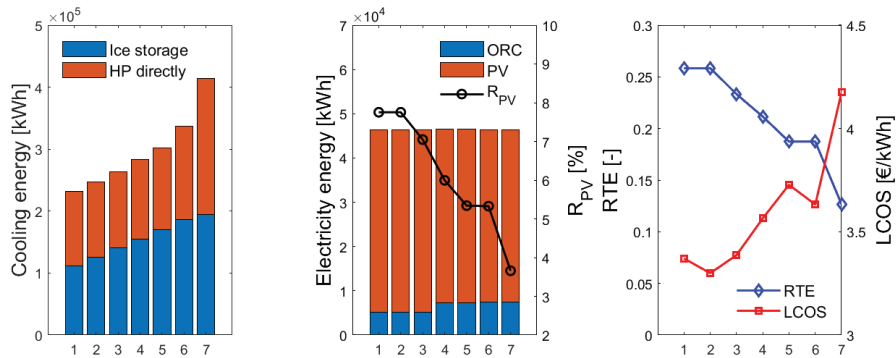


Figure 7. Performance comparison with various $CR_{elec}$ and $CR_{cooling}$

### 4.7  Improvement measure

In section 4.5, it was observed that the optimal $R_V$ differs significantly from the HP pressure ratio because of its large temperature difference. As a result, an electrical heater (EH) can be used instead of the HP condenser to produce hot water, allowing the HP to operate between ambient air and ice storage with a much smaller temperature difference. Simultaneously, as HP can produce more cooling capacity with a lower pressure ratio, ORC can be cooled by ice storage (glycol-water glide=5K), instead of well water. Thus, HP and ORC can reach a near pressure ratio and optimal $R_V$, so $R_V$ here is determined as a large value, 4.5. $T_{hot}$ has no impact on HP performance anymore so it can be set as 95°C for higher $\eta_{ORC}$. As other parameters remain the same as results of section 4.4, COP is 2.7 and $\eta_{ORC}$ is 9.5% with both compressor and expander efficiency close to 0.7. Its improved configuration is shown in Figure 8. The investment cost of EH refers to Pardillos-Pobo et al. (2023), and its nominal power is set as 130kW. Its instant power at each hour is:

$$\dot{W}_{EH} = \dot{W}_{PV,tot} - \dot{W}_{load} - \dot{W}_{HP} \tag{22}$$

This means that the EH operation priority order is the lowest after HP. The hourly variation of hot/ice storage is in equation (23) and (24), respectively:

37th INTERNATIONAL CONFERENCE ON EFFICIENCY, COST, OPTIMIZATION, SIMULATION AND ENVIRONMENTAL IMPACT OF ENERGY SYSTEMS, 30 JUNE - 4 JULY, 2024, RHODES, GREECE

437

$$\Delta E_{hot,sto} = \int_0^{3600} (\dot{Q}_{EH} - \dot{Q}_{ORC,ev})dt \tag{23}$$

$$\Delta E_{ice,sto} = \int_0^{3600} (\dot{Q}_{HP,ev} - \dot{Q}_{cooling} - \dot{Q}_{ORC,cd})dt \tag{24}$$



Figure 8. Configuration of improved reversible HP/ORC with EH

For fully covering demands, a feasible size of the improved configuration with EH is also listed in Table 2. Compared with No.7 without EH, the size of the PV array is half, and the size of other components are all reduced. As a result, its RTE is 0.1877, where $W_{EH}$ is added in the denominator of equation (15). Its LCOS is 2.29 €/kWh, which is 30.4% lower than No.2 without EH.

**Table 2:** System size with various coverage

| Designing No. | $CR_{elec}$ | $CR_{cooling}$ | $\dot{W}_{PV,nom}$/kW | $V_{S,cmp}$/cm³ | Hot/ice Sto./kWh |
|---|---|---|---|---|---|
| 1 (Without EH) | 95% | 70% | 400 | 1000 | 400 / 3500 |
| 2 (Without EH) | 95% | 75% | 400 | 1180 | 400 / 3500 |
| 3 (Without EH) | 95% | 80% | 440 | 1180 | 400 / 3500 |
| 4 (Without EH) | 99% | 85% | 490 | 1180 | 1200 / 3500 |
| 5 (Without EH) | 99% | 90% | 550 | 1180 | 1200 / 3500 |
| 6 (Without EH) | 99% | 95% | 550 | 1500 | 1800 / 3500 |
| 7 (Without EH) | 100% | 100% | 800 | 1500 | 2800 / 3500 |
| With EH | 100% | 100% | 400 | 1180 | 2500 / 3500 |

## 4.8 Design results

The performance of the reversible HP/ORC in No. 2&7 without EH and improvement with EH will be discussed. In one year, their performance is listed in Table 3. With an EH, nominal HP consumption power is much lower than that of No.2 without EH, so its full-speed HP hours are much more although their PV power is the same. Simultaneously, its HP evaporator generates more cooling due to more full-speed HP hours and higher COP, and thus the ice storage size can remain the same (Table 2), even though the ice storage covers both cooling demand and ORC consumption. The main difference between No. 2&7 is that the full-speed HP mode of No.2 is less, and the reduced-speed mode is more than that of No.7. The PV power in No.7 is twice as high as that in No.2, and the nominal HP consumption power is only 27% larger than that in No.2, so No.7 has more chance to reach the nominal condition of HP mode. All these designs have no full-speed ORC mode because No.2 doesn't need to 100% cover the electricity demand at full speed. In No.7 without EH and the design with EH, both of which fully cover the electricity demand, their nominal ORC power is higher than the peak power demand, so the expander never operates at the maximum speed. The hour of reversible HP/ORC stopping mode happens when there is no electricity demand or PV power, and ice storage covers the cooling demand.

**Table 3:** Comparison of operation performance

| Working mode | No.2 without EH | No.7 without EH | With EH |
|---|---|---|---|
| Carnot battery stopping time / hour | 92 | 92 | 92 |
| Full-speed heat pump time / hour | 642 | 1583 | 2398 |
| Reduced-speed heat pump time / hour | 3187 | 2273 | 1431 |
| Full-speed ORC time / hour | 0 | 0 | 0 |
| Reduced-speed ORC time / hour | 4839 | 4812 | 4839 |
| Nominal ORC production power / kW | 22.8 | 29.0 | 44.7 |
| Nominal HP consumption power / kW | 225.7 | 286.9 | 80.7 |
| Nominal ORC evaporator power / kW | 654.7 | 832.2 | 470.1 |
| Nominal ORC condenser power / kW | 615.7 | 782.6 | 399.0 |
| Nominal HP condenser power / kW | 277.9 | 353.2 | 219.7 |
| Nominal HP evaporator power / kW | 120.0 | 152.5 | 163.4 |
| COP | 1.23 | 1.23 | 2.72 |
| $\eta_{ORC}$ | 3.48% | 3.48% | 9.51% |

## 5    CONCLUSIONS

An off-grid Carnot battery (reversible HP/ORC) with a PV array is designed for the electricity and cooling demands of a family farm in Nigeria. As its food preservation temperature range is 0-5°C, glycol water solution is selected as secondary fluid for ice storage, and R152a is selected as working fluid. After analyzing the effects of pinch, the top temperature of the hot water tank, glides, and $R_V$ on COP as well as $\eta_{ORC}$, the size of the PV array, hot/ice storage, and reversible HP/ORC is determined in various coverage of demands. With the selected operation boundary (pinch=5K, hot water glide=15K, $T_{hot}$=87°C, glycol water glide=8K) and $R_V$=2, COP and $\eta_{ORC}$ reach 1.23 and 3.48%, respectively. Under part coverage sizing ($CR_{elec}$=95%, $CR_{cooling}$=75%), RTE and LCOS are 104.1% higher and 21% lower than those in full coverage sizing respectively. The improvement design, where an EH replaces HP for charging hot storage and ORC is cooled by ice storage instead of well water, gets COP of 2.72 and $\eta_{ORC}$ of 9.51% with a different boundary ($T_{hot}$=95°C, glycol water glide=5K) from that without EH. It improves the performance significantly and reduces the size and investment cost when demands are fully covered. The next step is to investigate the performance of a configuration where the second fluid of the HP condenser can be switched between water cooled by ambient air and hot water from hot storage, so HP can operate in two modes either for better cooling or charging hot storage. Moreover, additional renewable energy resources such as wind energy and batteries will be integrated to reduce reliance on PV arrays, especially during periods of weak solar intensity. This strategic diversification aims to lower $N_{PV}$ and thus reduce the initial investment cost.

## NOMENCLATURE

| | | |
|---|---|---|
| A | area | (m$^2$) |
| C | cost | (€) |
| c | specific heat | (J/kg·K) |
| COP | coefficient of performance | (-) |
| E | total energy | (J) |
| f | derating factor | (-) |
| GI | global irradiance | (W/m$^2$) |
| L | latent heat | (J/kg) |
| M | mass | (kg) |
| N | number | (-) |
| $\dot{Q}$ | heat transfer rate | (W) |
| R | ratio | (-) |

37th INTERNATIONAL CONFERENCE ON EFFICIENCY, COST, OPTIMIZATION, SIMULATION AND ENVIRONMENTAL IMPACT OF ENERGY SYSTEMS, 30 JUNE - 4 JULY, 2024, RHODES, GREECE

439

| Re | Reynolds number | (-) |
| T | temperature | (K) |
| t | time | (s) |
| V | volume | $(cm^3)$ |
| W | work | (J) |
| $\dot{W}$ | power | (W) |
| α | temperature coefficient of power | (-) |
| η | efficiency | (-) |

**Subscript**

| CB | Carnot battery |
| cd | condenser |
| cell | cell |
| comp | compressor |
| cooling | cooling demand |
| ev | evaporator |
| ex | exhaust |
| exp | expander |
| hot | hot water |
| hp | heat pump |
| inv | invert |
| nom | nominal condition |
| ORC | organic Rankine cycle |
| ref | refrigeration |
| STC | standard test condition |
| sto | storage |
| su | supply |
| tot | total |
| w | water |

## REFERENCES

Benato, A., Stoppato, A., 2018, Pumped thermal electricity storage: a technology overview, *Thermal Science and Engineering Progress*, 6, 301-315.

Dumont O., 2017, Investigation of a heat pump reversible in an organic Rankine cycle and its application in the building sector.

Dumont O., Lemort V., 2019, Thermo-technical approach to characterize the performance of a reversible heat pump/organic Rankine cycle power system depending on its operational conditions, *ECOS 2019*.

Dumont O., Frate G. F., Pillai A., et al., 2020, Carnot battery technology: A state-of-the-art review, *Journal of Energy Storage*, 32: 101756.

Dumont O., Lemort V., 2020a, Modelling of a thermally integrated Carnot battery using a reversible heat pump/organic Rankine cycle, *ECOS 2020*.

Dumont O., Lemort V., 2020b, Mapping of performance of pumped thermal energy storage (Carnot battery) using waste heat recovery, *Energy*, 211: 118963.

Dumont O., Thome O., Lemort V., 2023, Methodology for the sizing of a Carnot battery based on a Rankine cycle and application to a 10 kWe system for district heating application, *ECOS 2023*.

Iqbal, Q., Fang, S., Zhao, Y., et al., 2023, Thermo-economic assessment of sub-ambient temperature pumped-thermal electricity storage integrated with external heat sources, *Energy Conversion and Management*, 285, 116987.

Laterre, A., Dumont, O., Lemort, V., et al., 2024, Is waste heat recovery a promising avenue for the Carnot battery? Techno-economic optimisation of an electric booster-assisted Carnot battery integrated into different data centres, *Energy Conversion and Management*, 301: 118030.

37th INTERNATIONAL CONFERENCE ON EFFICIENCY, COST, OPTIMIZATION, SIMULATION AND ENVIRONMENTAL IMPACT OF ENERGY SYSTEMS, 30 JUNE - 4 JULY, 2024, RHODES, GREECE

https://doi.org/10.52202/077185-0037                    440

Lemort V., Quoilin S., Cuevas C., et al. 2009, Testing and modeling a scroll expander integrated into an Organic Rankine Cycle, *Applied Thermal Engineering*, 29(14-15): 3094-3102.

Martinek, J., Jorgenson, J., McTigue, J. D., 2022, On the operational characteristics and economic value of pumped thermal energy storage, *Journal of Energy Storage*, 52, 105005.

Migliari L., Petrollese M., Cau G., et al., 2024, Techno-economic assessment and grid impact of Thermally-Integrated Pumped Thermal Energy Storage (TI-PTES) systems coupled with photovoltaic plants for small-scale applications, *Journal of Energy Storage*, 77: 109898.

Pardillos-Pobo, D., González-Gómez, P. A., Laporte-Azcué, M., et al., 2023, Thermo-economic design of an electric heater to store renewable curtailment in solar power tower plants, *Energy Conversion and Management*, 297, 117710.

Poletto C., Dumont O., De Pascale A., et al., 2024, Control strategy and performance of a small-size thermally integrated Carnot battery based on a Rankine cycle and combined with district heating, *Energy Conversion and Management*, 302: 118111.

Scharrer D., Bazan P., Pruckner M., et al., 2022, Simulation and analysis of a Carnot Battery consisting of a reversible heat pump/organic Rankine cycle for a domestic application in a community with varying number of houses, *Energy*, 261: 125166.

Smith, K., Saxon, A., Keyser, M., et al., 2017, Life prediction model for grid-connected Li-ion battery energy storage system, *2017 American Control Conference (ACC)*, IEEE, 2017: 4062-4068.

Song, X., Zhu, T., Liu, L., et al., 2018, Study on optimal ice storage capacity of ice thermal storage system and its influence factors, *Energy Conversion and Management*, 164: 288-300.

Steger D., Regensburger C., Eppinger B., et al., 2020, Design aspects of a reversible heat pump-Organic Rankine cycle pilot plant for energy storage, *Energy*, 208: 118216.

Tassenoy R., Dumont O., Lemort V., et al., 2022, Experimental Investigation of A Thermally Integrated Carnot Battery Using A Reversible Heat Pump/Organic Rankine Cycle: Influence Of System Charge On Performance Of The Reversible Scroll Compressor/Expander And Global Performance, *19th International Refrigeration and Air Conditioning Conference. Purdue University*, 2022: 1-11.

Torricelli N., Branchini L., De Pascale A., et al., 2023, Optimal Management of Reversible Heat Pump/Organic Rankine Cycle Carnot Batteries, *Journal of Engineering for Gas Turbines and Power*, 145(4): 041010.

UNFCCC, 2018, The Paris Agreement, *Paris Climate Change Conference - November 2015*

United Nations, 1998, Kyoto Protocol to the United Nations Framework Convention on Climate Change. New York, USA.

**ACKNOWLEDGEMENT**

37th INTERNATIONAL CONFERENCE ON EFFICIENCY, COST, OPTIMIZATION, SIMULATION AND ENVIRONMENTAL IMPACT OF ENERGY SYSTEMS, 30 JUNE - 4 JULY, 2024, RHODES, GREECE

441

https://doi.org/10.52202/077185-0037